Dynamic PON Consolidation Using MEMS Optical Switches for Energy Efficient Optical Line Terminals Using Real Operator Data

1st Mirco Börner
Technische Hochschule Mittelhessen
35390 Gießen, Germany
mirco.boerner@ei.thm.de

2nd Kristof Obermann
Technische Hochschule Mittelhessen
35390 Gießen, Germany
kristof.obermann@ei.thm.de

3rd Carmen Mas-Machuca
University of the Bundeswehr Munich
85579 Neubiberg, Germany
cmas@unibw.de

***Abstract*—This work presents a dynamic Passive Optical Network (PON) consolidation approach using low-cost Micro-Electro-Mechanical Systems (MEMS) optical switches to deactivate unneeded Optical Line Terminal (OLT) ports or even complete line cards. Our simulation framework employs an algorithm considering individual port loads, Optical Network Unit (ONU) limits, and topology restrictions with real OLT architecture and power consumption data. Using 24-hour traffic traces from 2986 access connections provided by a major German network operator, we evaluate 2x2 and 4x4 MEMS switch groups on Gigabit-capable PON (GPON) and 10-Gigabit-capable Symmetric PON (XGS-PON) systems with splitting ratios of 1:32, 1:64, and 1:128. Results demonstrate energy savings of 21.94–29.23 % for GPON and up to 39.49 % for XGS-PON under current traffic conditions. For projected future traffic, the analysis reveals that XGS-PON maintains stable savings through x20 traffic scaling and continues to provide meaningful savings even at further scaling. The optical switching groups additionally provide redundancy for failure protection and operational flexibility for load balancing without physical re-wiring.**

I. Introduction

With more than 143 million fiber to the home/building (FTTH/B) subscribers in the EU39 region alone in 2024 [1], Passive Optical Networks (PONs) have become a dominant access technology. As a consequence of their large-scale deployment, improving the energy efficiency of the PON technology is a globally critical challenge, particularly since Information and Communications Technology accounted for 4–6 % of global electricity consumption in 2020 [2]. At the same time, there is an increasing demand for high capacity PON technologies, which are typically accompanied by higher power consumption, as applications such as 4k, 8k, Virtual Reality (VR), Augmented Reality (AR), etc. are on the rise and drive the demand for increased network capacity [3]. Therefore, network operators face a contradiction in the dimensioning of PON, since when looking at the traffic profiles of residential customers, we already see a significant discrepancy between network utilization during the day and night [4]. This makes cost- and energy effective network dimensioning challenging as operators need to design networks that are able to handle peak traffic loads, while over-provisioning results in wasted energy during low traffic phases.

A possible approach to reduce the power consumption at the Optical Line Terminal (OLT)-side is to introduce line rate utilization dependent PON consolidation and thus deactivation of unneeded ports or even the whole line card. This concept was shown in [5] where the authors proposed to implement optical switches interconnecting the OLT line cards and PONs to be able to consolidate the PONs on fewer line cards during low utilization phases and put the freed line cards to sleep. An analytical model of energy saving potential was proposed using semi-markov chains and self-similar traffic simulations were conducted for architectures using $N \times N$ and cascaded 2×2 optical switches. However, there are a couple limitations to the work, as the actual port-level structure was neglected and only the common line card capacity was taken into account. Also, the work only investigated the theoretical potential at given traffic loads, disregarding actual utilization patterns. This aspect was considered in an earlier work [6] in which the potential of PON consolidation was estimated based on aggregated traffic at all members of Amsterdam Internet Exchange. However, this work also disregarded port-level granularity. Furthermore, representing daily OLT utilization as a relative reference to maximum traffic in an aggregated node does not adequately describe the real PON, neglecting the actual absolute utilization of the network. A comparable approach was also presented for long-reach systems in [7], where PONs could be consolidated using a Remote Channel Combine/Split utilizing multiple wavelengths.

Building on the previous works, we address the provisioning discrepancy through dynamic, port-level PON consolidation enabled by low-cost Micro-Electro-Mechanical Systems (MEMS) optical switches. In contrast to prior studies, which considered only aggregated line card capacities, our approach models port-level constraints such as individual port loads, Optical Network Unit (ONU) limits, and switching topology constraints. Furthermore, we base our evaluation on real traffic traces from individual connections provided by a large German network operator. This allows us to validate energy savings

This work was supported by the Federal Ministry of Research, Technology and Space (BMFTR) Germany as part of the PONGO project (Grant ID 16KIS2078).

under realistic conditions. Using this simulation framework with 24-hour traffic data, we demonstrate possible energy savings of 21.94–29.23 % for current Gigabit-capable PON (GPON) deployments. We show that our approach maintains significant savings even under traffic growth scenarios migrating to 10-Gigabit-capable Symmetric PON (XGS-PON), while enabling failure protection through the inherent redundancy of the optical switching groups.

II. Methodology

A. OLT Architecture

We model commercial OLT systems based on real configuration data. The baseline GPON OLT system consists of 6 line cards with 16 GPON ports each, combining a total of 96 PON ports. Each port provides 2.488 Gbit/s downstream and 1.244 Gbit/s upstream capacity, with a maximum of 128 ONUs per port according to the GPON recommendation [8]. This OLT system will be compared to an XGS-PON system from the same vendor, consisting of 6 line cards with 8 XGS-PON ports each. Each XGS-PON port provides 9.953 Gbit/s in upstream and downstream and can serve a maximum of 256 ONUs [9]. Although these configurations represent actual OLTs deployed in current access networks, the power consumption might vary depending on the specific OLT models. However, we expect that the relative savings achieved through PON consolidation will be applicable to comparable systems.

To enable dynamic PON consolidation with cross line card flexibility, we propose two switching concepts that allow for the potential deactivation of complete line cards. Commercially available latching MEMS switches are used due to their advantageous properties such as low insertion loss, high reliability, and low power consumption [10]. The first concept forms 48 2×2 switch groups (Fig. 1) across the 96-port GPON OLT, each combining two 1×2 MEMS switches [11] with a 1:2 splitter, allowing flexible 2×2 interconnection between two OLT ports and two PONs. The second concept forms 24 4×4 switch groups with 1×4 switches [12] and 1:4 splitters (Fig. 1). This enables flexible 4×4 interconnection between four OLT ports and four PONs and the consolidation of up to four PONs on a single port. Switch groups are formed to enable cross line card consolidation. Line cards are partitioned into groups of at most N cards (where N is the switch size). Each $N\times N$ switch group then connects the ports of all line cards within one line card-group. When a group contains fewer than N line cards, each switch can connect multiple ports per line card. For instance, with 4×4 switch groups and 6 line cards, 4 cards form one group while the remaining 2 cards form another. In addition, both concepts provide redundant switching paths for fail-safe operation.

The integration of optical switches introduces additional physical layer considerations. Each switch has an insertion loss of approximately 0.6–1 dB. The effective doubling or quadrupling of the splitting ratio introduces an estimated additional 3 dB or 6 dB of optical loss, respectively. For conventional PON systems, this requires careful network planning to maintain optical budget margins and limits the possible switch group size. However, emerging coherent PON technologies could offer the capability to dynamically adjust modulation schemes, potentially recovering $\sim$ 3 dB during low-traffic periods [13].

TABLE I
OLT COMPONENT POWER CONSUMPTIONS

Component	GPON		XGS-PON	
	Number	Power total percentage	Number	Power total percentage
Core	1	55.67 %	1	40.59 %
Line Card	6	22.21 %	6	46.30 %
Port	96	22.12 %	48	13.11 %

B. Traffic Data Generation

Our simulation uses real traffic data provided by a major German network operator. The data set comprises time-series measurements from 2986 individual user connections, captured at 1-second intervals. This data set reflects user behavior patterns that include diurnal variations, peak usage periods, and characteristic asymmetry between downstream and upstream traffic.

To generate representative PON instances, we implement a comprehensive sampling approach. For each PON, we sampled individual user connections from the pool of available connections. We configured all PONs to be occupied by 100 %, to represent fully provisioned networks and therefore the worst case regarding utilization. The number of users per PON is determined by the specified splitting ratio (1:32, 1:64, 1:128). Individual user time series are aggregated to form the total PON traffic profile. Since the user data represent actual Ethernet level traffic data, we apply PON specific overhead factors before simulation. For GPON, an additional overhead of 7 % is assumed as a worst case scenario according to [14]. For XGS-PON an overhead of 15 % is assumed [15], [16].

The simulation has an initial configuration where the generated PONs are uniformly distributed across the available ports, with each port serving exactly one PON.

C. Power Model

Our power model divides the OLT power consumption into components shown in Table I, based on real data for GPON and XGS-PON OLTs. Power consumptions are presented as percentages of the total OLT power consumption to provide confidentiality. The core includes chassis components, fabric cards, uplink card, power supply, fans, and the uplink Small Form-factor Pluggables (SFPs). Line cards can be powered down when all associated ports are inactive. Port power consumption encompasses the individual PON SFPs. Ports can be individually deactivated when no PONs are connected.

The power consumption characteristics are defined based on their specific data sheets. We use latching switches for energy efficient operation. The 2×2 groups consist of two individual 1×2 MEMS switches. This switch has no static power consumption. The switching process requires two control pulses for a combined pulse width of 50 ms and a total switching

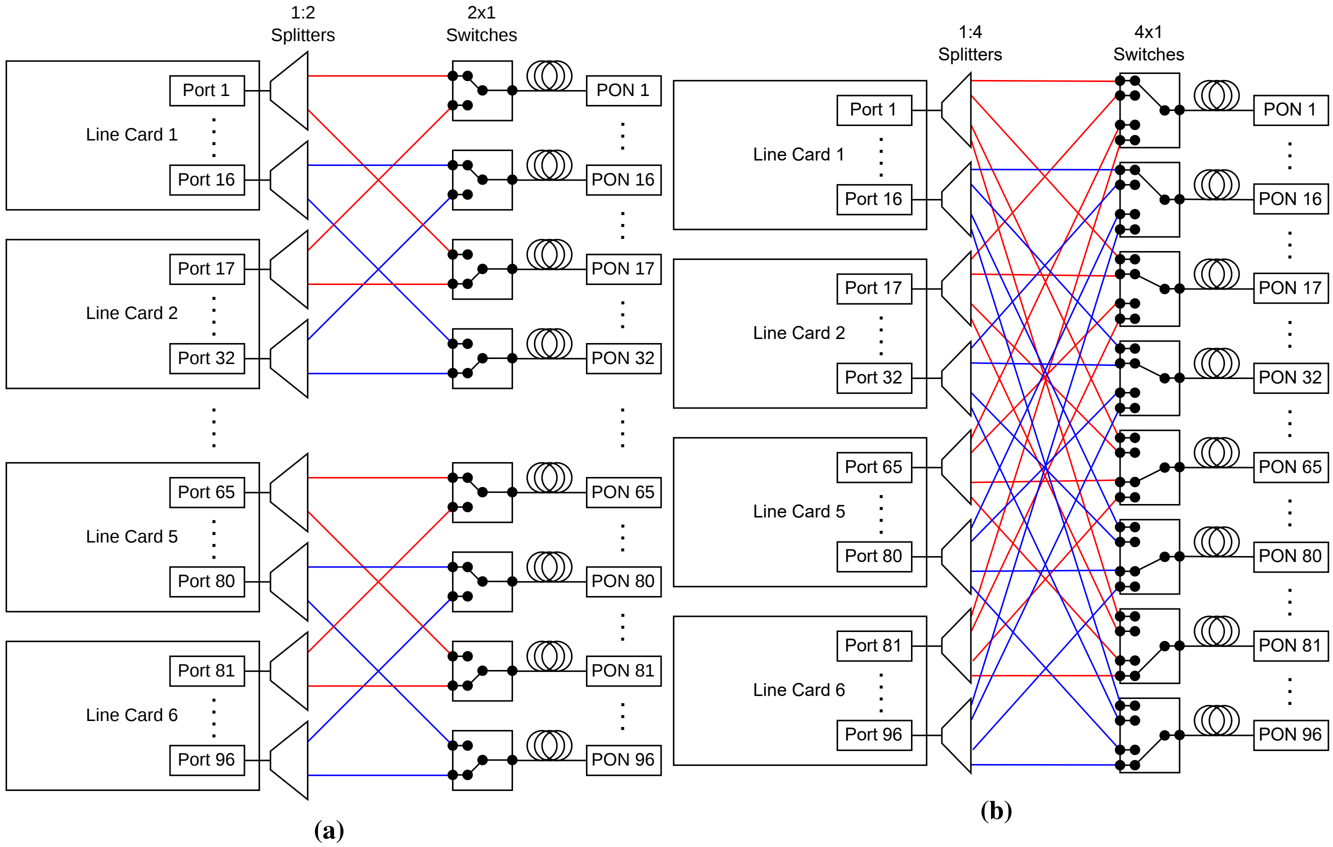

Fig. 1. PON consolidation concepts with (a) 2×2 switch groups and (b) 4×4 switch groups.

energy per switch of 13.6 mWs [11]. The 4×4 switch groups employ four 1×4 MEMS switches. The power consumptions differ from the 2×2 groups as each 1×4 switch has a static power consumption of 15 mW and a single switching process consumes 20 mWs given a pulse width of 40 ms [12].

The total power consumption of the system over time is computed as shown in Eq. (1), where P_{core} is the static power consumption of the core components, $P_{LC,i}(t)$ represents time dependent line card power consumption for each line card i out of N, and $P_{port,i}(t)$ as well as $P_{switch,i}(t)$ denote the time dependent power consumption for each port and switch i, respectively. The reference power is given as the total OLT power consumption from Table I.

$$P_{total}(t) = P_{core} + \sum_{i=1}^{N} P_{LC,i}(t) + \sum_{i=1}^{M} (P_{port,i}(t) + P_{switch,i}(t)) \quad (1)$$

D. Switching Algorithm

The core of our simulation approach is the switching algorithm, which is executed at each simulation step and has the objective to minimize the number of active ports.

In the first step, the algorithm identifies and resolves strained ports serving two or more consolidated PONs to prevent network performance degradation. A port is classified as strained when its utilization U_{port} exceeds the threshold T_{upper}. Port utilization is defined in Eq. (2), where L_{US} and L_{DS} are the port loads in upstream and downstream and C_{US} and C_{DS} are the port capacity in upstream and downstream, respectively.

$$U_{port} = max\left(\frac{L_{DS}}{C_{DS}}, \frac{L_{US}}{C_{US}}\right) \quad (2)$$

To ensure stable operation and avoid too frequent switching events, which would unnecessarily increase power consumption, the algorithm uses a listening mechanism similar to [5]. A port must remain in the strained state for a duration of $t_{listen,over}$ before triggering a migration action. When this action is activated, the PON with the highest traffic load at the strained port is identified and migrated to a port in the same switch group that is able to accept the PON without reaching the strained condition itself. The $t_{listen,over}$ timer is then reset if the port is no longer strained. If no suitable port exists, an inactive port can be activated to accommodate the migrated PON.

The underloaded ports are then identified to reduce power consumption. A port is classified as underloaded when U_{port} falls below the threshold T_{lower}. The algorithm applies a listening time mechanism, where the underloaded condition must persist for $t_{listen,under}$ to allow PON consolidation. During PON consolidation, PONs from underutilized ports are migrated to already active ports within the same switch group that have sufficient capacity, prioritizing migrations that maximize the potential for a line card to have all ports deactivated. The $t_{listen,under}$ timers of the involved ports are then reset if they are no longer underutilized.

In the last step, the algorithm performs a line card consolidation check. If the ratio of active line cards to total line cards exceeds the ratio of active ports to total ports, PONs are migrated from ports on sparsely utilized line cards to ports on line cards with more active ports within the same switch group. All ports without connected PONs are powered down. Line cards without active ports may also be powered down to achieve further energy savings. Each switch is not allowed to undergo more than one switching operation per timestep to prevent oscillatory behavior and reduce switching related overhead.

To illustrate the switching behavior, consider a 4×4 switch group connecting ports A–D across four line cards, where port A serves three consolidated PONs and port B serves one PON. If the utilization U_{port} of port A exceeds T_{upper} for $t_{listen,over}$, the algorithm identifies the PON with the highest traffic load on port A and migrates it to port B, provided port B can accommodate the additional load without exceeding T_{upper}. If no active port has sufficient capacity, an inactive port within the same switch group is activated. In contrast, if port B's utilization falls below T_{lower} for $t_{listen,under}$, its PON is migrated to port A and port B is powered down, provided port A has sufficient capacity. If this causes all ports on port B's line card to become inactive, the entire line card is powered down as well.

E. Parameter Optimization

The switching algorithm depends on the four parameters T_{upper}, T_{lower}, $t_{listen,over}$, and $t_{listen,under}$. To identify robust parameters, we employ a systematic two stage optimization approach. To determine the ideal thresholds in the first step, we conduct simulations with a parameter sweep varying $T_{upper} \epsilon \{60\,\%, 70\,\%, 80\,\%, 90\,\%\}$ and $T_{lower} \epsilon \{20\,\%, 30\,\%, 40\,\%, 45\,\%\}$ with the listen parameters kept constant to 1 s. As a performance metric to balance energy efficiency with operational stability, we define a trade-off ratio. In Eq. (3) N is the total number of ports, while ES are the energy savings achievable with this particular parameter combination and $OL_{port,i}$ is the percentage of time each port is overloaded and reaches its maximum utilization.

$$\textit{Trade-off-Ratio} = \frac{ES}{\frac{1}{N}\sum_{i=1}^{N} OL_{port,i}} \quad (3)$$

With the ideal configuration identified as $T_{upper} = 90\,\%$ and $T_{lower} = 20\,\%$, the listen times are evaluated in the same way, with parameters varied $t_{listen,over} \epsilon \{1\,\text{s}, 2\,\text{s}, 4\,\text{s}, 6\,\text{s}, 8\,\text{s}, 10\,\text{s}\}$ and $t_{listen,under} \epsilon \{1\,\text{s}, 2\,\text{s}, 4\,\text{s}, 6\,\text{s}, 8\,\text{s}, 10\,\text{s}\}$. This results in ideal parameters being determined as $t_{listen,over} = 1\,\text{s}$, which is the minimum value for the given time resolution, and $t_{listen,under} = 10\,\text{s}$.

III. Results

The evaluation is structured in two parts. First, an analysis for the presented GPON OLT with the real traffic traces is performed to demonstrate the fundamental energy saving potential under current traffic conditions. Second, cross-generation scalability is examined, investigating how the concept performs across different PON generations and future traffic scaling scenarios.

A. GPON current traffic traces

To evaluate the potential energy savings under current traffic conditions, simulations are performed for the GPON OLT serving 96 fully occupied PONs using different switch group sizes (2×2 and 4×4) with varying base splitting ratios (1:32 and 1:64).

The 2×2 switch groups achieve an average $22.16\,\%$ reduction in total power consumption, by consolidating two 1:32 PONs into a single port operating at an effective 1:64 splitting ratio, allowing inactive ports and entire line cards to be powered down. The 4×4 switch groups deliver energy savings of $29.23\,\%$ by consolidating up to four 1:32 PONs.

For current unscaled traffic profiles, the system maintains complete consolidation throughout the observation period without requiring reconfiguration as traffic loads remain sufficiently low, resulting in a constant reduction of power consumption. Therefore, optical switches primarily enable a more flexible network configuration, additionally providing fault protection mechanisms rather than frequent dynamic switching operations. Configurations with 1:64 base splitting ratio and 2×2 switch groups show the same energy savings and traffic behaviors as for the 1:32 base splitting ratio. However, since the standardized splitting ratio for GPON is limited to 1:128 [8], 4×4 switch groups do not increase energy efficiency for the 1:64 base split.

For cost-sensitive deployments, the 2×2 switch groups with 1:32 base split PONs could achieve substantial savings while minimizing additional optical attenuation with commercially available and mass-produced 1×2 latching MEMS switches. Beyond energy savings, the optical switching configuration provides safety margins and operational flexibility for traffic spikes and failure scenarios, as the switches enable load rebalancing without physical re-wiring of fiber.

B. Cross Generation Scalability

To evaluate the long-term viability of optical switch-based consolidation, we examine scalability under projected future traffic scenarios. Traffic is scaled with different factors ranging from $\times 1$ to $\times 100$, analyzing both GPON and XGS-PON configurations using the OLT data from Table I.

For the GPON OLT, Fig. 2 shows the results for $\times 10$ scaled traffic data with 4×4 switch groups and 1:32 base PON split. The individual curves represent the power consumption of each OLT component group as a percentage of the full active OLT reference power. Unlike the static consolidation for unscaled traffic, the results for $\times 10$ scaling show clear diurnal patterns and daily energy savings of $22.78\,\%$. During nighttime hours, the PONs are consolidated powering down four of the six line cards, while daytime traffic forces port-reactivation. Because of the port-granular algorithm, even the activation of a single port on a previously inactive line

TABLE II

GPON MEAN ENERGY SAVINGS FOR DIFFERENT SCALING FACTORS

Scaling Factor	2 × 2 Switch		4 × 4 Switch	
	1:32	1:64	1:32	1:64
×1	22.16 %	22.16 %	29.23 %	21.94 %
×5	22.15 %	20.60 %	28.35 %	15.95 %
×10	18.85 %	10.33 %	22.78 %	8.29 %
×15	13.48 %	6.08 %	16.59 %	4.77 %
×20	10.70 %	4.10 %	12.91 %	3.92 %
×40	6.19 %	2.13 %	7.27 %	1.75 %
×60	4.53 %	1.72 %	5.46 %	1.17 %
×80	4.02 %	1.49 %	4.65 %	0.98 %
×100	3.49 %	1.18 %	3.77 %	0.75 %

card requires powering up the entire card, creating jumps in OLT power consumption. Table II summarizes the energy savings for GPON configurations. Energy savings decrease as traffic increases since more ports must remain active during peak hours. The 4 × 4 switch configuration outperforms the 2 × 2 configuration for 1:32 splits, as the 4 × 4 switch groups allow for more effective consolidation and additional flexibility in migrating PONs between ports. However, this advantage shrinks as maximum port utilization is approached. This superior performance must be weighed against increased implementation costs and additional optical attenuation. Configurations with 1:64 or even 1:128 splitting ratios exhibit faster decreasing savings for scaled traffic rates because of the higher traffic per PON. If the split ratio does not allow the consolidation of more than two PONs given the ONU limit with respect to the PON standard, the 2 × 2 switch groups are superior to the 4 × 4 groups. However, it must be noted that as a base architecture higher split ratios are obviously more energy efficient than lower ones.

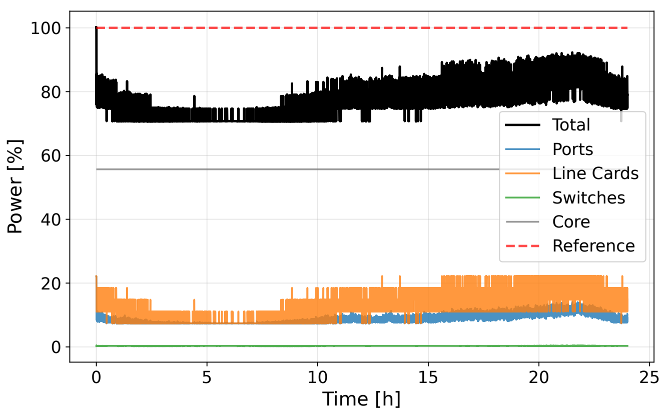

Fig. 2. Power consumption components as percentage of the full active reference power for a GPON OLT with 1:32 splitting ratio and 4 × 4 switch groups under ×10 scaled traffic.

The savings at higher scaling factors must be interpreted with caution. As traffic load increases, consolidated ports may reach their maximum capacity despite the migration mechanism of the switching algorithm. To quantify this effect, the overload ratio is defined as the mean percentage of time that ports exceed their maximum capacity, averaged across all ports. Table III lists the lowest scaling factor at which the overload ratio first exceeds 0.5 % for each configuration. For GPON, 2 × 2 1:64 base split configurations begin to experience overload periods for about 1.96 % of time at ×10 scaling, reaching 12.95 % at ×15 scaling. For 1:32 configurations, notable overload periods emerge at ×15 scaling (1.57 %) and increase substantially at ×20 negating practical applicability. At these high scaling factors, the energy savings in Table II are achieved predominantly during off-peak hours when utilization is still low enough for consolidation.

Fig. 3 presents energy savings in both GPON and XGS-PON configurations as a function of traffic scaling factors ranging from ×1 to ×100, encompassing base splitting ratios of 1:32, 1:64, and 1:128, with 2 × 2 and 4 × 4 switch groups. It can be observed that the higher port capacity of XGS-PON significantly extends the viability of optical switch-based consolidation. XGS-PON with 1:32 base splitting ratio and 2 × 2 switches maintains 29.68 % savings through ×20 scaling with negligible overload occurrence. The 4 × 4 groups achieve 39.49 % energy savings at ×1 traffic and still 11.02 % at ×100 scaling, although 13.49 % overload is reached at ×100. For the 1:128 base splitting ratio, only XGS-PON is viable, and results for 2 × 2 and 4 × 4 are nearly identical as only two-PON consolidation is possible.

TABLE III

OVERLOAD PERIODS FOR SCALING THRESHOLDS

Standard	Split	2 × 2 Switch		4 × 4 Switch	
		Scaling	Overload	Scaling	Overload
GPON	1:32	×15	1.57 %	×15	1.53 %
GPON	1:64	×10	1.96 %	×10	2.02 %
XGS-PON	1:32	×60	2.31 %	×60	2.32 %
XGS-PON	1:64	×40	2.91 %	×40	3.10 %
XGS-PON	1:128	×20	1.04 %	×20	1.07 %

It should be noted that the absolute energy savings depend on OLT hardware characteristics, specifically the power consumption ratio between core, line cards, and SFPs. Although based on real data, the results may vary for different OLT models. Several practical implementation aspects require further investigation. The simulation does not model actual switching times beyond the use for power consumption calculations and neglects necessary PON connection recovery procedures following switching events. Real deployment would require adequate protocol development to minimize service interruption. PON consolidation inherently increases effective splitting ratios, affecting PON power budgets. Network planning must account for this. However, coherent PON technologies could offer a mitigation strategy by dynamically adjusting modulation schemes to recover approximately 3 dB of optical budget [13]. Alternatively, optical amplifiers can be deployed to maintain power budget margins, although this introduces additional cost and power consumption.

IV. CONCLUSION

This paper presents a dynamic PON consolidation approach using MEMS optical switches to reduce OLT power

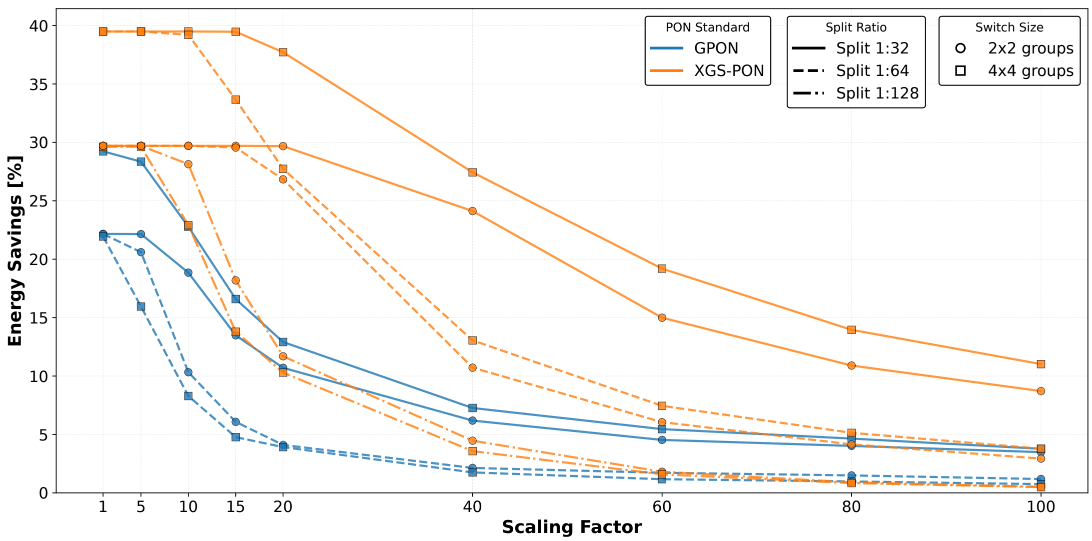

Fig. 3. Energy savings vs. data rate scaling factors for GPON and XGS-PON

consumption by enabling port and line card sleep modes during periods of low network utilization. In contrast to prior analytical studies, our simulation framework incorporates OLT port-level granularity and real access traffic data from 2986 user connections provided by a major German network operator. The evaluation demonstrates substantial energy saving potential across multiple configurations. For current GPON deployments with 1:32 splitting ratios, the 2×2 switch groups achieve $22.16\,\%$ energy savings, while the 4×4 groups reach $29.23\,\%$. The scalability analysis reveals that XGS-PON significantly extends the viability of optical switch-based consolidation in future traffic growth scenarios. With a 1:32 splitting ratio and 2×2 switch groups, XGS-PON maintains stable savings of $29.68\,\%$ through $\times 20$ traffic scaling and still achieves savings at larger scaling factors, depending on the configuration. The results indicate that, given the cost and optical budget, 4×4 switches provide great savings for split ratios of up to 1:32 for GPON and 1:64 for XGS-PON. For higher splitting ratios, due to optical budget constraints, 2×2 switches appear to be ideal. Beyond energy efficiency, the optical switching infrastructure provides operational benefits including inherent path redundancy for failure protection and the capability for dynamic load re-balancing without physical fiber modifications. Because of its potential to mitigate optical path loss, optical switch-based consolidation could also represent a viable strategy for future coherent PON technologies.

References

[1] FTTH council europe, "EUROPEAN FTTH/B MARKET PANORAMA 2025," Accessed: 14 December 2025. [Online]. Available: https://www.ftthcouncil.eu/resources/all-publications-and-assets/2358/european-ftth-b-market-panorama-2025

[2] A. Ross and L. Christie, "Energy consumption of ICT," Accessed: 19 March 2025. [Online]. Available: https://post.parliament.uk/research-briefings/post-pn-0677/

[3] S. Strube Martins and C. Wernick, "Regional differences in residential demand for very high bandwidth broadband internet in 2025," *Telecommunications Policy*, vol. 45, no. 1, p. 102043, 2021.

[4] L. Wang, J. Zhang, Z. Zhang, and J. Zhang, "Analytic Network Traffic Prediction Based on User Behavior Modeling," *IEEE Networking Letters*, vol. 5, no. 4, pp. 208–212, 2023.

[5] M. Taheri, J. Zhang, and N. Ansari, "Design and Analysis of Green Optical Line Terminal for TDM Passive Optical Networks," *Journal of Optical Communications and Networking*, vol. 8, no. 4, pp. 221–228, 2016.

[6] J. Zhang, T. Wang, and N. Ansari, "Designing energy-efficient optical line terminal for TDM passive optical networks," in *34th IEEE Sarnoff Symposium*, 2011, pp. 1–5.

[7] H. Feng, C.-J. Chae, A. V. Tran, and A. Nirmalathas, "Cost-Effective Introduction and Energy-Efficient Operation of Long-Reach WDM/TDM PON Systems," *Journal of Lightwave Technology*, vol. 29, no. 21, pp. 3135–3143, 2011.

[8] International Telecommunication Union, "Gigabit-capable passive optical networks (GPON): General characteristics," Apr. 3, 2008, Accessed: 19 March 2025. [Online]. Available: https://handle.itu.int/11.1002/1000/9379

[9] ——, "10-Gigabit-capable symmetric passive optical network (XGS-PON)," Feb. 22, 2023, Accessed: 19 March 2025. [Online]. Available: https://handle.itu.int/11.1002/1000/15133

[10] I. Plander and M. Stepanovsky, "MEMS optical switch: Switching time reduction," *Open Computer Science*, vol. 6, 10 2016.

[11] Agiltron Inc., "MEMS Ultra-Mini 1x2, 2x2 Latching Series Fiber Optical Switch," accessed: 11 December 2025. [Online]. Available: https://agiltron.com/dlc/specs/MEMS%20U-Mini%20Series%20latching%20Switch.pdf

[12] ——, "MEMS 1x4 Mini Latching Series Fiber Optic Switch," accessed: 11 December 2025. [Online]. Available: https://agiltron.com/dlc/specs/MEMS%201x3%201x4%20Latching%20Switch.pdf

[13] G. Di Rosa, O. Jovanovic, M. Kuipers, and J.-P. Elbers, "Demonstration of Low-Complexity Triple-Rate Coherent PON Achieving Up to 200 Gbit/S Symmetric Data Rates," in *2025 European Conference on Optical Communications (ECOC)*, 2025, pp. 1–4.

[14] O. Marmur and E. Shraga, "GPON: the next big thing in optical access networks," in *Network Architectures, Management, and Applications*, S. J. Ben Yoo, Kwok-wai Cheung, Yun-Chur Chung, and Guangcheng Li, Eds., vol. 5282. SPIE, 2004, pp. 199–209.

[15] M. I. Nashiruddin, N. Solihah, and M. A. Nugraha, "Capability Assesment of the XGS-PON Optical Network Termination for Residential Customer," in *2021 13th International Conference on Information Technology and Electrical Engineering (ICITEE)*, 2021, pp. 34–39.

[16] K. A. Mat Sharif, N. A Ngah, A. Ahmad, K. Khairi, Z. A. Manaf, and D. Tarsono, "Demonstration of XGS-PON and GPON Co-Existing in the Same Passive Optical Network," in *2018 IEEE 7th International Conference on Photonics (ICP)*, 2018, pp. 1–3.